

Hollow NiCo₂O₄ Nanofibers as Sulphur Host Materials for High-Performance Lithium-Sulphur Batteries

Yunfeng Lin^{1,2,*}, Yigao Miao^{1,2}

¹ Lishui University, Lishui, Zhejiang, 323000, China.

² Key Laboratory of Digital Design and Intelligent Manufacturing for Creative Cultural Products of Zhejiang Province, Lishui, Zhejiang, 323000, China.

*E-mail: yunfenglinzj@tom.com

Received: 3 January 2020 / Accepted: 2 February 2020 / Published: 10 April 2020

Cobaltate plays an important role in many applications, such as photocatalysis and water purification. However, few works have reported about the employment of cobaltate in energy storage systems. As we all know, the lithium-sulfur batteries suffer from severe capacity fade during the electrochemical cycles due to the shuttle effect of the polysulfide products. In our work, we design hollow NiCo₂O₄ nanofibers as host materials for elemental sulfur in lithium-sulfur batteries. The unique hollow nanofiber structure could provide sufficient space for the storage of the soluble polysulfide and inhibit the migration of the polysulfide products. Moreover, the chemical bond of Ni-S is proved to exist after electrochemical cycles, demonstrating chemical relationship between the NiCo₂O₄ and soluble polysulfide. As a result, the as-prepared hollow NiCo₂O₄-S composites exhibit high capacity and excellent cycling stability.

Keywords: Cobaltate, Polysulfide, Li-S battery, Migration, Capacity

1. INTRODUCTION

The breaking news that Goodenough won the Nobel Prize indicates that researches on the new energy storage systems are more and more attractive of the scientists all over the world [1]. Goodenough has made great contributions to the lithium-ion batteries, who found the suitable cathode materials for the lithium-ion batteries [2, 3]. During the past decades, many achievements have been obtained for improving the electrochemical performance of the lithium-ion batteries, such as NCM [4], NCA [5] and Si-based anode materials [6]. However, the traditional lithium-ion batteries have low capacity and energy density, and they fail to satisfy the high energy density needs of the electric vehicles and other electric devices [7, 8]. Therefore, it is urgent for us to look for new energy storage systems with high energy density and capacity at the same time [9].

Among various energy storage systems, lithium-sulfur batteries are considered as one of the most promising candidates to replace the traditional lithium-ion batteries due to their high specific capacity (1675 mAh g^{-1}) and energy density (2600 Wh Kg^{-1}) [10, 11]. Many teams and individuals have been devoted themselves to study the lithium-sulfur batteries [12]. However, as so far, the applications of lithium-sulfur batteries are still hindered due to many problems, which are caused by the poor cycle performance [13]. The poor cycle stability of the lithium-sulfur batteries is ascribed to the severe shuttle effect of the soluble polysulfide during the electrochemical process [14]. The polysulfide products will be migrated from the cathode side to the anode side [15]. Therefore, we have to deal with this issue to improve the cycle stability of the lithium-sulfur batteries.

To deal with this problem, many efforts have been made, including developing advanced host materials for the lithium-sulfur batteries [16], finding new electrolyte system [17] and protecting the lithium anode [18]. For these methods, designing suitable host materials is the most efficient way to inhibit the shuttle effect of the polysulfide. At the beginning, various carbon materials were prepared and developed as host materials. These carbon-based sulfur composites display superior electrochemical performance. However, the carbon materials only could provide non-polar adsorption for the polysulfide. Therefore, the inhibition for the migration of polysulfide is limited. After that, metal oxides were used in the lithium-sulfur batteries. The as-prepared composite cathode can efficiently inhibit the migration of polysulfide due to presence of polar adsorption between metal oxide and polysulfide [19]. There are few works about the employment of cobaltate in the lithium-sulfur batteries.

Based on the above theme, in our work, we prepared hollow NiCo_2O_4 nanofibers as host materials for element sulfur in lithium-sulfur batteries. The unique hollow nanofiber structure can provide sufficient space for the storage of the soluble polysulfide and inhibit the migration of the polysulfide products. Moreover, the chemical bond of Ni-S is proved to exist after electrochemical cycles, demonstrating chemical relationship between the NiCo_2O_4 and soluble polysulfide. As a result, the as-prepared HNCO-S composites exhibit high capacity and excellent cycling stability.

2. EXPERIMENTAL

2.1. Preparation of NiCo_2O_4 nanofibers

Solid NiCo_2O_4 nanofibers were prepared via two-step reactions. Typically, 1.2 mol $\text{Ni}(\text{NO}_3)_2$ and 1.8 mol $\text{Co}(\text{NO}_3)_2$ were dissolved into 100 mL H_2O . Then, 5 mol hexamethy lenetetramine was added into the above mixture under stirring for 30 min. After that, the obtained pink solution was transferred into Teflon-lined autoclave and heated at 120°C for 12 h. After naturally cooling down to room temperature, the final product was vacuum dried at 60°C for 12 h. For comparison, the hollow NiCo_2O_4 nanofibers were also prepared via heating the solid NiCo_2O_4 nanofibers at 300°C for 3 h.

2.2. Preparation of NiCo_2O_4 -S composites

The NiCo_2O_4 -S composites were synthesized by heating the mixture of pure sulfur and solid

NiCo₂O₄ nanofibers and hollow NiCo₂O₄ nanofibers. The mixture was prepared by mixing pure sulfur and NiCo₂O₄ nanofibers with a ratio of 3:1. After that, the mixture was uniformly grounded for 20 min. Then, the mixture was transferred into tube furnace at 155°C for 12 h in Ar atmosphere. Finally, the mixture was continuously heated at 200°C for 3 h to remove the unstable sulfur in the composites. The hollow NiCo₂O₄-S composites were prepared by the same method as like the preparation of solid NiCo₂O₄-S composites.

2.3. Materials Characterization

The material structures were all characterized via corresponding equipment. The morphology of the samples was observed by using scanning electronic microscopy (SEM, Phenom LE) with vacuum degree of 10⁻⁴-10⁻⁵ mmHg. The internal structure was displayed via employing transmission electronic microscopy (TEM, JEM-F200). The crystal structure of the samples was tested by using X-Ray Diffractometer (XRD, D8 Advance) with 2 theta of 20-60°. The active content (S%) in the composites was determined via using thermal gravimetric analyzer (TGA, TG-DTA 8121) at Ar atmosphere with heating rate of 5°C/min.

2.4. Electrochemical Performance

Firstly, electrode slurry was prepared by mixing active materials, super carbon and PVDF with a mass ratio of 90:5:5 by using NMP as solvent. The slurry was grounded for 20 min until the slurry was uniform. Then, the prepared electrode slurry was uniformly coated on the surface of the Al film and dried at 60°C for 24h. After that, the electrode film was pouched into circle electrode with diameter of 15 mm. Finally, the coin 2032 half batteries were assembled in the glove box filled with Ar atmosphere. For the preparation of coin 2032 half batteries, the as-prepared active electrode films were used as cathode. The lithium was used as anode. The separator type was Clegard 2400. The electrolyte was consisted of 1M Lithium difluoromethylsulfonamide (LITFSI) with 1, 3-dioxolane (DOL) and dimethyl ether (DME)=1:1. The discharge and charge profiles were tested at battery tested of LANDCT2001A between 1.8 V and 2.8 V.

3. RESULTS AND DISCUSSION

The different morphologies of NiCo₂O₄ were prepared via controlling the heating temperature. As shown in Figure 1a and b, the as-prepared NiCo₂O₄ materials all exhibit nanofiber structure. However, it can be seen that NiCo₂O₄ shows solid nanofiber structure (Figure 1a). For the figure 1b, the as-prepared NiCo₂O₄ displays hollow nanofiber structure, which is beneficial for the soakage of element sulfur into the hollow space. More importantly, the unique hollow nanofiber structure could act as tankage for the polysulfide products which are produced during the discharging process of the lithium-sulfur batteries. In detail, the electrochemical performance of the HNCO-S composites was

tested by coin batteries. The electrochemical results are shown in Figure 5 and 6.

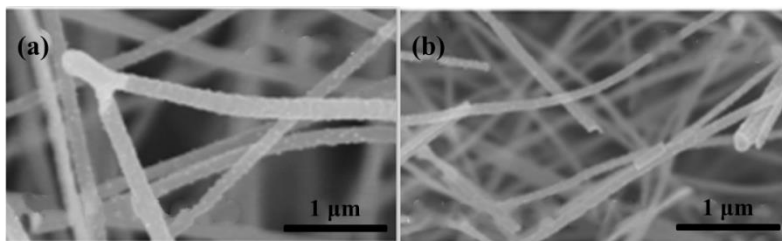


Figure 1. SEM images of (a) solid NiCo₂O₄ nanofibers. (b) hollow NiCo₂O₄ nanofibers.

Figure 2a shows the XRD patterns of the solid NiCo₂O₄ nanofibers and hollow NiCo₂O₄ nanofibers. As shown in Figure 2a, the as-prepared solid NiCo₂O₄ nanofibers and hollow NiCo₂O₄ nanofibers show similar diffraction peaks from 20° to 60°. This indicates the successful preparation of the NiCo₂O₄ nanofibers materials. The diffraction peaks are located at 42°, 46° and 53°, respectively. They are corresponding to the crystal plane of (110), (121) and (010), indicating the high purity of the NiCo₂O₄ nanofibers [20]. Figure 2b displays the XRD patterns of pure sulfur and HNCO-S composites. It can be clearly seen that the HNCO-S composites show similar diffraction peaks with the pure sulfur materials except for the intensity of the diffraction peaks [21]. This is ascribed to the coverage of NiCo₂O₄ on the pure sulfur. The difference between the pure sulfur and HNCO-S composites is that the as-prepared HNCO-S composites exhibit weak diffraction peaks. In all, the HNCO-S composites were successfully prepared and could be developed as cathode materials for the lithium-sulfur batteries.

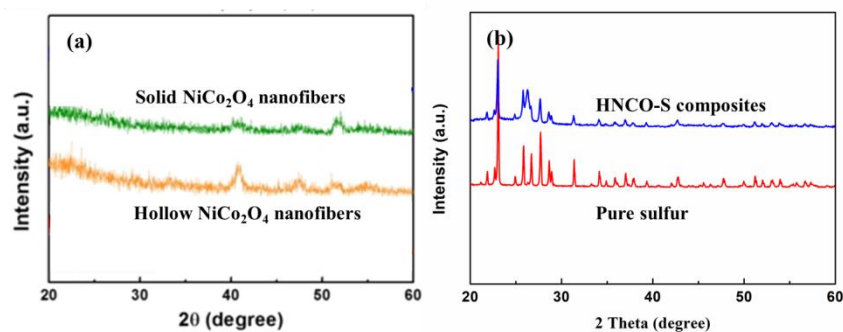


Figure 2. (a) and (b) XRD patterns of the solid NiCo₂O₄ nanofibers, hollow NiCo₂O₄ nanofibers, pure sulfur and HNCO-S composites.

Figure 3a shows the SEM image of the hollow NiCo₂O₄ nanofibers. As shown in Figure 3a, the HNCO exhibits hollow nanofiber structure with a diameter of 80-100 nm. Figure 3b is the TEM image of the HNCO, further demonstrating the hollow nanofiber structure. After heating the HNCO with element sulfur, the HNCO-S composites are obtained. As shown in Figure 3c, the HNCO-S composites show different morphology with the pure HNCO materials. It could be clearly observed that the surface of the HNCO is occupied with the sulfur particles. Besides, there are sulfur particles in the

hollow nanofiber structure [22]. To confirm the result, TME image for the HNCO-S composites were conducted. As shown in Figure 3d, the sulfur particles can be observed in the hollow nanofiber structure. To further investigate the element in the HNCO-S composites, elemental mapping was tested. As shown in Figure 3e-h, it can be seen that elements Ni, Co and S are uniformly distributed into the whole HNCO-S composites. As a result, the HNCO-S composites were successfully prepared and could be used as cathode materials for the lithium-sulfur batteries. The uniform composites could ensure the total capacity release during the electrochemical process [23].

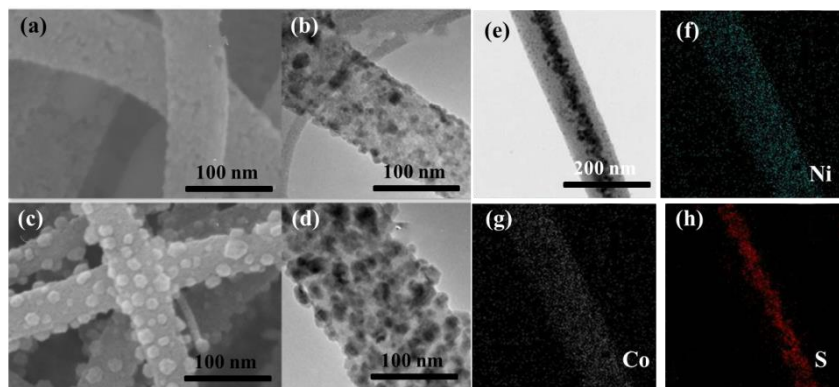


Figure 3. (a) and (c) SEM images of the HNCO and the HNCO-S composites, respectively. (b) and (d) TEM images of the HNCO and the HNCO-S composites, respectively. (e-h) TEM image of HNCO-S composites and the corresponding elemental mapping of the elements Ni, Co and S.

The severe shuttle effect of polysulfide is the main reason for the fast capacity fade for the lithium-sulfur batteries. Therefore, it is important for the cathode materials which could inhibit the shuttle effect. To prove the adsorption ability of the hollow NiCo_2O_4 nanofibers, adsorption test was conducted in a Li_2S_6 solution by using HNCO, as shown in Figure 4a. The pristine Li_2S_6 solution is yellow color, which is consistent with the reported works. After adding HNCO into the pristine Li_2S_6 solution, the yellow color disappears, confirming the superior adsorption ability of the hollow NiCo_2O_4 nanofibers. Moreover, the XPS of the cathode materials after electrochemical cycles was conducted. As shown in Figure 4b, for the cycled HNCO-S composites, it can be seen that Ni-S chemical bond was existed in the HNCO-S composites, which was located at 169.2 eV. Besides, there are also two peaks at 167.1 eV and 163.0 eV, respectively. They are corresponding to the S $2p_{1/2}$ and S $2p_{3/2}$, respectively. The sulfur content in the HNCO-S and SNCO-S composites is determined via TG analysis. As shown in Figure 4c, it can be seen that the sulfur contents are 65% and 66%, respectively.

Based the above results, it can be concluded that the as-prepared HNCO-S composites possesses superior adsorption ability for the soluble polysulfide. Therefore, the electrochemical performance of the HNCO-S composites must be excellent. Figure 5a shows the constant discharge and charge profiles of the HNCO-S composites. It can be seen that the initial specific capacities of the HNCO-S composites are 1389, 1206, 1046, 901, 752, 625 mAh g^{-1} at 0.1 C, 0.2 C, 0.5 C, 1 C, 2 C and 3 C, respectively. Even at high rate of 5C, the specific capacity is as high as 468 mAh g^{-1} . However, for

the SNCO-S composites, it suffers from severe capacity fading with the increase of the current rates. Besides, it can be observed that obvious polarization emerged with the current increase. The severe polarization was caused by the poor electronic conductivity of the SNCO-S composites. Moreover, the SNCO-S composites failed to inhibit the migration of the polysulfide in the lithium-sulfur battery [24].

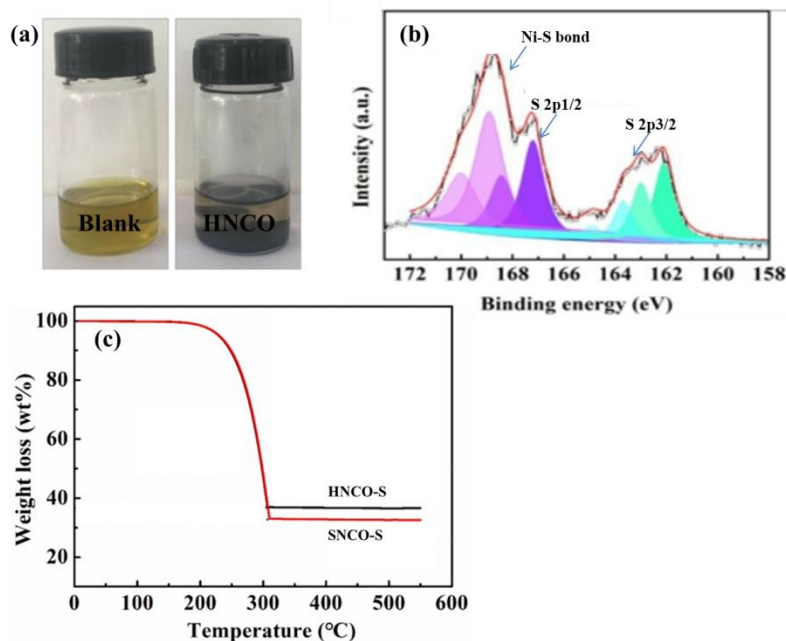


Figure 4. (a) Li_2S_6 adsorption in DOL/DME solution by using HNCO. (b) XPS study of HCON-S composites after electrochemical cycles. (c) TG analysis of the HNCO-S and SNCO-S composites.

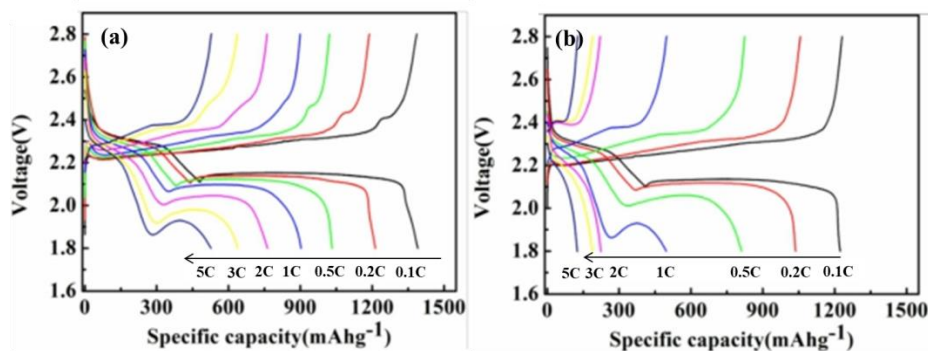


Figure 5. (a) and (b) Discharge and charge profiles of the HNCO-S and SNCO-S composites at different current densities from 0.1 C to 5 C.

Figure 6a displays the CV curves of the HNCO-S composites between 1.8 V and 2.8 V at scanning rate of 0.1 mV s^{-1} . First, there are two reduction peaks at 2.26 V and 2.05 V, respectively. These peaks are related to the transformation from S_8 rings to highly soluble polysulfide, then to Li_2S_2 and Li_2S , respectively. This is a two-step reaction, which is different from the traditional cathode materials. Besides, one oxidation peak at 2.35 V could be clearly observed, which is attributed to the chemical reaction from Li_2S to S_8 molecule. Moreover, it can be seen that the CV curves from 1st to 5th

overlap well, indicating superior reversibility. To investigate the cycle stability of the HNCO-S composites, cycle performance was tested at 0.2 C for 100 cycles. As shown in Figure 6b, the as-prepared HNCO-S composites exhibited initial specific capacity of 1206 mAh g⁻¹ at 0.2 C. After 100 cycles, the specific capacity still remained at 1008 mAh g⁻¹. This excellent cycle stability can be ascribed to the presence of the hollow NiCo₂O₄ nanofibers, which could efficiently inhibit the migration of the soluble polysulfide. As a result, the cycle stability can be improved. Therefore, it can be inferred that the HNCO-S composites can be used as cathode materials for the lithium-sulfur batteries [25].

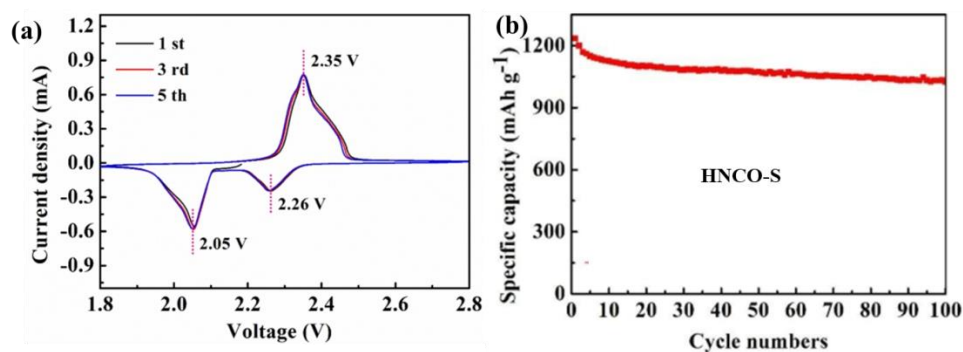


Figure 6. (a) CV curves of the HNCO-S composites. (b) Cycle performance of the HNCO-S composites at 0.2 C for 100 cycles.

Based above results, it can be concluded that the as-prepared HNCO-S composites exhibit excellent cycle stability and high specific capacity at the high current density. Furthermore, to show the superior electrochemical performance, a table was made for comparing the electrochemical performance of the HNCO-S composites with other similar cathode materials for the lithium-sulfur batteries. As listed in Table 1, the HNCO-S composites show initial capacity of 1206 mAh g⁻¹ at 0.2 C. After 100 cycles, the capacity of the HNCO-S composites is as high as 1008 mAh g⁻¹. As for the reported cathode materials, it can be seen that they suffers from severe capacity fade during the cycles. Therefore, the superior electrochemical performance is attributed to the unique hollow structure, which could improve the electron conductivity and inhibit the shuttle effect of the polysulfide.

Table 1. Electrochemical performance of the cathode materials for the lithium-sulfur batteries.

Composites	Rate	Initial Capacity	Cycle Stability	Reference
Sulfur/halloysite	0.1 C	985	603	26
Co ₃ S ₄ /MnS	0.2 C	1109	960	27
NC@CeO ₂	0.2 C	1006	823	28
HNCO-S	0.2 C	1206	1008	This work

4. CONCLUSIONS

In summary, different morphologies of NiCo₂O₄ were successfully prepared and designed as host materials for the lithium-sulfur batteries. The electrochemical results indicated that the as-

prepared HNCO-S composites exhibited higher specific capacity and superior cycling stability than the SNCO-S composites. The excellent electrochemical performance was attributed to the unique hollow nanofiber structure, which could storage the polysulfide. In addition, the chemical adsorption between the HNCO and polysulfide could further ensure the stability of the polysulfide at the cathode side. Therefore, the as-prepared HNCO-S composites exhibited an initial specific capacity of 1206 mAh g⁻¹ at 0.2 C. After 100 cycles, the specific capacity still remained at 1008 mAh g⁻¹.

ACKNOWLEDGEMENT

We thank the financial support from the Lishui University.

References

1. Y. Hu, W. Chen, T. Y. Lei, Y. Jiao, H. B. Wang, X. P. Wang, G. F. Rao, X. F. Wang, B. Chen and J. Xiong, *Nano Energ.*, 68 (2020) 104373.
2. X. Jiao, P. H. Ji, B. Shang, Q. Peng, G. C. Xi, T. B. Zeng, Y. J. Zou and X. B. Hu, *Solid State Ionics*, 344 (2020) 115150.
3. S. Y. Zhao, X. H. Tian, Y. K. Zhou, B. Ma and A. Natarajan, *J. Energ. Chem.*, 46 (2020) 22.
4. Y. P. Li, T. Y. Jiang, H. Yang, D. Lei, X. Y. Deng, C. Hao, F. X. Zhang and J. L. Guo, *Electrochim. Acta*, 330 (2020) 135311.
5. C. Huang, Y. Zhou, H. B. Shu, M. F. Chen, Q. Q. Liang, S. X. Jiang, X. L. Li, T. T. Sun, M. Y. Han, Y. J. Zhou, J. Jian and X. Y. Wang, *Electrochim. Acta*, 329 (2020) 135135.
6. Z. Wu, L. Yuan, Q. R. Han, Y. J. Lan, Y. Zhou, X. H. Jiang, X. P. Ouyang, J. W. Zhu, X. Wang and Y. S. Fu, *J. Power Sources*, 450 (2020) 227658.
7. M. F. Chen, X. M. Zhao, Y. F. Li, P. Zeng, H. Liu, H. Yu, M. Wu, Z. H. Li, D. S. Shao, C. Q. Miao, G. R. Chen, H. B. Shu, Y. Pei and X. Y. Wang, *Chem. Eng. J.*, 385 (2020) 123905.
8. M. D. Walle, M. Y. Zhang, K. Zeng, Y. J. Li and Y. N. Liu, *Appl. Surf. Sci.*, 497 (2019) 143773.
9. Y. Y. Geng, Z. P. Ma, L. Su, L. Sang, F. Ding and G. J. Shao, *J. Alloys Compd.*, 815 (2020) 152189.
10. L. Zhang, B. Wu, Q. F. Li and J. F. Li, *Appl. Surf. Sci.*, 484 (2019) 1184.
11. C. Wang, Y. K. Yi, H. P. Li, P. W. Wu, M. T. Li, W. Jiang, Z. G. Chen, H. M. Li, W. S. Zhu and S. Dai, *Nano Energ.*, 67 (2020) 104253.
12. Y. Yan, J. C. Xie, Y. Zhao, Y. Zhang, N. Cui, C. Li and C. Hao, *J. Alloys Compd.*, 805 (2019) 733.
13. J. W. Guo and M. S. Wu, *Electrochim. Acta*, 327 (2019) 135028.
14. S. J. Chen, Y. Ming, B. C. Tan and S. Y. Chen, *Electrochim. Acta*, 329 (2020) 135128.
15. S. J. Ruan, Z. C. Huang, W. D. Cai, C. Ma, X. J. Liu, J. T. Wang, W. M. Qiao and L. C. Ling, *Chem. Eng. J.*, 385 (2020) 123840.
16. J. F. Wu, S. Y. Ding, S. H. Ye and C. Lai, *J. Energ. Chem.*, 42 (2020) 27.
17. M. S. Kim, M. S. Kim, V. Do, Y. Xia, W. Kim and W. L. Cho, *J. Power Sources*, 422 (2019) 104.
18. L. L. Fan, M. Li, X. F. Li, W. Xiao, Z. W. Chen and J. Lu, *Joule*, 3 (2019) 361.
19. W. D. Li, Z. Chen, D. Z. Wang, Z. J. Gong, C. M. Mao, J. Liu, H. R. Peng, Z. H. Zhang and G. C. Li, *J. Power Sources*, 435 (2019) 226778.
20. J. L. Cheong, A. Hamid and J. Y. Ying, *Nano Energ.*, 66 (2019) 104114.
21. C. L. Wang, L. S. Sun, X. X. Wang and L. M. Wang, *Carbon*, 153 (2019) 691.
22. J. Y. Wang, W. J. Wang, Y. G. Zhang, Z. Bakenov, Y. Zhao and X. Wang, *Mater. Lett.*, 255 (2019) 126581.
23. J. Leng, Z. X. Wang, X. H. Li, H. J. Guo, T. Li and H. M. Liang, *Electrochim. Acta*, 244 (2017) 154.
24. C. Huang, T. T. Sun, H. B. Shu, M. F. Chen and X. Y. Wang, *Electrochim. Acta*, 334 (2020)

135658.

25. R. Y. Yan, M. Oschatz and F. X. Wu, *Carbon*, 161 (2020) 162.
26. Y. X. Pei, Y. X. Wang, Y. Darraf, A. Y. Chang, H. Zhao, X. Liu, J. G. Liu, Y. Lvov and S. N. Wang, *J. Power Sources*, 450 (2020) 227698.
27. Y. P. Li, T. Y. Jiang, H. Yang, D. Lei, X. Y. Deng, C. Hao, F. X. Zhang and J. L. Guo, *Electrochim. Acta*, 330 (2020) 135311.
28. W. T. Qi, W. Jiang, F. Xu, J. B. Jia, C. Yang and B. Q. Cao, *Chem. Eng. J.*, 382 (2020) 122852.

© 2020 The Authors. Published by ESG (www.electrochemsci.org). This article is an open access article distributed under the terms and conditions of the Creative Commons Attribution license (<http://creativecommons.org/licenses/by/4.0/>).